

# Perturbing the Cochlea

C. Elliott Strimbu,<sup>1, a)</sup> Elika Fallah,<sup>1, b)</sup> and Elizabeth S. Olson<sup>1, 2, c)</sup>

<sup>1)</sup>*Department of Otolaryngology Head and Neck Surgery, Columbia University, New York, NY, USA*

<sup>2)</sup>*Department of Biomedical Engineering, Columbia University, New York, NY, USA*

<sup>a)</sup>*Corresponding author: CE Strimbu ces2243@cumc.columbia.edu*

<sup>b)</sup>*Electronic mail: ef2516@columbia.edu*

<sup>c)</sup>*Electronic mail: eao2004@columbia.edu*

**Abstract.** Cochlear mechanics can be studied by perturbing physiological and mechanical components of the organ of Corti (OC) and observing the outcomes. We have combined OCT-based *in vivo* vibrometry at the base of the gerbil cochlea with pharmacological perturbation of different components of the amplifier, including transiently abolishing the endocochlear potential (EP) with intravenous furosemide and inhibition of somatic electromotility by introducing sodium salicylate into the perilymphatic space. Vibrations in healthy cochleae were measured before and for several hours after the pharmacological perturbations to characterize the loss and recovery of the active process. DPOAEs were monitored and, for the furosemide experiments, EP and local cochlear microphonic observations were available from a previous set of experiments in our lab. For both salicylate and furosemide perturbations, outer hair cell sub-best-frequency (BF) nonlinearity recovered before the BF peak. In the salicylate studies intra-OC changes in the motion occurred as the cochlea recovered. In the furosemide experiments, the recovery of the BF peak occurred many minutes after EP recovery. Normal transduction currents have been shown to be necessary to maintain stereocilia morphology and loss of EP might transiently damage hair cell stereocilia, leading to the delayed recovery of functional amplification of the BF peak. We explored this hypothesis with histological studies of bundle morphology following furosemide. These observations have not yielded clear-cut results – bundle morphology usually appeared normal, although important changes might have occurred at more subtle levels. In sum, the constellation of factors that together give rise to cochlear amplification include EP, electromotility and transducer nonlinearity, and as-yet unidentified factors that must be properly aligned to give rise to a functioning whole.

## INTRODUCTION

The endocochlear potential, the  $\sim +80$  mV potential in scala media, is essential for normal cochlear amplification. In previous studies on furosemide, we reversibly eliminated the EP by an intravenous (IV) injection of furosemide in gerbil and measured the basal local cochlear microphonic (LCM) [1], the vibrations of the OC complex (OCC) [2], and distortion product otoacoustic emissions (DPOAEs). The EP recovered over  $\sim 40$  minutes while vibrations, LCM and DPOAEs recovered later,  $\sim 2$  hours post injection. Vibration was measured using optical coherence tomography (OCT). The axis of OCT measurement had both longitudinal and transverse components, and the measured motion was a combination of these [3].

In a second set of experiments, we transiently blocked OHC electromotility by introducing millimolar sodium salicylate into the scala tympani using a trans-round window membrane application, and monitored DPOAEs and OCC vibration. In the salicylate experiments we expanded the OCT vibration methodology employed in the furosemide study by constructing areal maps of the motion by taking a series of one-dimensional vibration measurements across the nearly radial field of view. The axis of OCT measurement was similar in the salicylate and furosemide experiments.

Following both furosemide and salicylate treatment, vibration amplitudes were diminished with basilar membrane (BM) vibrations resembling those of a passive cochlea, showing linear growth and a loss of the best frequency (BF) peak. The OHC region, some  $60 \mu\text{m}$  deeper in the cochlear partition also showed decreased amplitudes and a loss of the BF peak, but in contrast to the BM, its vibrations retained broad-band nonlinearity at frequencies below BF following both furosemide and salicylate. Recovery of the BF peak occurred in both studies over hours, taking longer following salicylate.

Vélez-Ortega *et al.* found that normal transduction currents are necessary to maintain stereocilia morphology [4]. We hypothesized that the loss of EP following IV furosemide will thus damage hair cell stereocilia and may in part explain the delayed recovery (after EP recovery) of cochlear amplification. In the new results presented here, we investigate the effect of IV injection of furosemide on the morphology of the OHC bundles by *ex vivo* imaging of the OHC bundles using scanning electron microscopy (SEM). Other new results presented here are *in vivo* areal maps of the vibration of the OCC during recovery from furosemide, to compare to our previously reported vibration maps following salicylate. All experiments were performed in young adult gerbils.

## METHODS

Experimental protocols were approved by the Columbia University Institutional Animal Care And Use Committee. Details of the surgery, OCT-based vibrometry, and introduction of furosemide and salicylate have been published [1, 2, 5, 6]. In brief, adult gerbils were anesthetized with ketamine, sodium pentobarbital, and buprenorphine and the left auditory bulla was exposed ventrally and opened. Furosemide, 100 mg/kg, was injected intravenously in the left femoral vein. In the salicylate experiments, 5  $\mu\text{L}$  of 50 mM sodium salicylate in artificial perilymph was deposited on the round window membrane and passively diffused into scala tympani. In the cochlear base, the extracellular salicylate concentration should rapidly reach an equilibrium concentration of  $\sim 2.5 - 5 \mu\text{M}$ , sufficient to block somatic electromotility [7].

A Tucker Davis Technologies D-to-A and A-to-D system running at 97656.25 S/s was used to generate the acoustic signals and to monitor the ear canal pressure. Stimuli were broad-band zwuis complexes in which a number of frequencies,  $N = 15$  in these experiments, were presented simultaneously. The frequencies are chosen such that they are linearly independent up to third order; thus there are no harmonics or second- or third-order distortion products in the frequency complex itself, and each sinusoidal component was assigned a random phase so that the total pressure amplitude is  $\sim \sqrt{N}$  higher than each primary in the complex. Stimuli were presented from 50 or 60 – 80 dB SPL (where 0 dB SPL  $\equiv 20 \mu\text{Pa}$ ) at each component.

DPOAEs were measured in response to swept two tone,  $f_1$  and  $f_2$ , stimuli where  $f_2$  was varied from 1 to 48 kHz,  $f_1$  and  $f_2$  were held in a fixed ratio of  $f_2/f_1 = 1.2$ , and both frequencies were presented at 50 and 70 dB SPL. The prominent  $2f_1 - f_2$  DPOAE served as a real-time measure of general cochlear condition. Baseline DPOAEs were consistent with healthy cochleae; the loss of the DPOAEs at 50 dB and sharp reduction at 70 dB immediately after treatment was used to assess the efficacy of the drug delivery and the recovery of the DPOAEs as a function of time indicated the recovery of cochlear amplification.

For vibrometry, the OCC was imaged through the intact round window membrane near the  $\sim 25 - 28$  kHz location. Measurements were performed with a ThorLabs Telesto III OCT system with a central wavelength of  $\sim 1300$  nm. The lateral resolution is set by the optics and is  $\sim 10 \mu\text{m}$  when measuring in water with an index of refraction  $n = 1.3$ . The axial resolution is set by the wavelength and bandwidth of the light source; the distance between adjacent axial pixels is  $2.7 \mu\text{m}$  in water. The OCT's line camera was locked to the TDT system clock to acquire time-locked 1-dimensional Ascans, or Mscans, which are then analyzed to find the motion of structures along the OCT axis of measurement. The time waveforms of motion at pixels of local maxima in the Ascans, which correspond to anatomical structures in the OCC, were determined by spectral domain phase microscopy and the amplitude and phases of the motion were then determined by Fourier analysis. Before and after each vibration measurement, the system took two dimensional scans, or Bscans, of the OCC and the two images were compared to check for drift in the preparation. Two dimensional, or areal, maps of the vibrations were measured by taking sequential Mscans in  $10 \mu\text{m}$  steps across an approximately radial section of the OCC. Linear interpolation was applied to these coarse maps to construct vibration maps that had the same number of pixels as the structural Bscans. This procedure is explained in more detail in Fig.1.

In each experiment, two sets of baseline recordings (DPOAEs and vibrometry measurements) were taken prior to pharmacological treatment. In the furosemide experiments, DPOAEs and vibration measurements were taken immediately after the injection was completed and at subsequent times for up to five hours post injection. In the salicylate study, we applied the sodium salicylate solution into the round window space and allowed the solution to passively diffuse into scala tympani for at least 10 minutes before wicking off the solution and washing with fresh artificial perilymph. DPOAE-grams were measured in 10 minute intervals to check for a loss the DPOAEs evoked by the 50 dB primaries. The DPOAE and vibrometry measurements were then repeated approximately every 20 minutes for several hours post treatment.

For SEM histology, gerbils were anesthetized and DPOAE thresholds were measured before and after furosemide injection to confirm the loss of the EP [1]. In order to observe the state of the stereocilia soon after the EP had dropped, the gerbil was euthanized minutes after the confirming DPOAE measurement. Cochleae were extracted, fixed in 2.5% glutaraldehyde supplemented with 2 mM of  $\text{CaCl}_2$ , dehydrated in graded series of ethanol, critical point dried from liquid  $\text{CO}_2$ , sputter coated with 5 nm platinum, and imaged with a ZEISS VP SEM. Control imaging was done in gerbils without furosemide injection. Electron high tension of the SEM (EHT) was 5 kV.

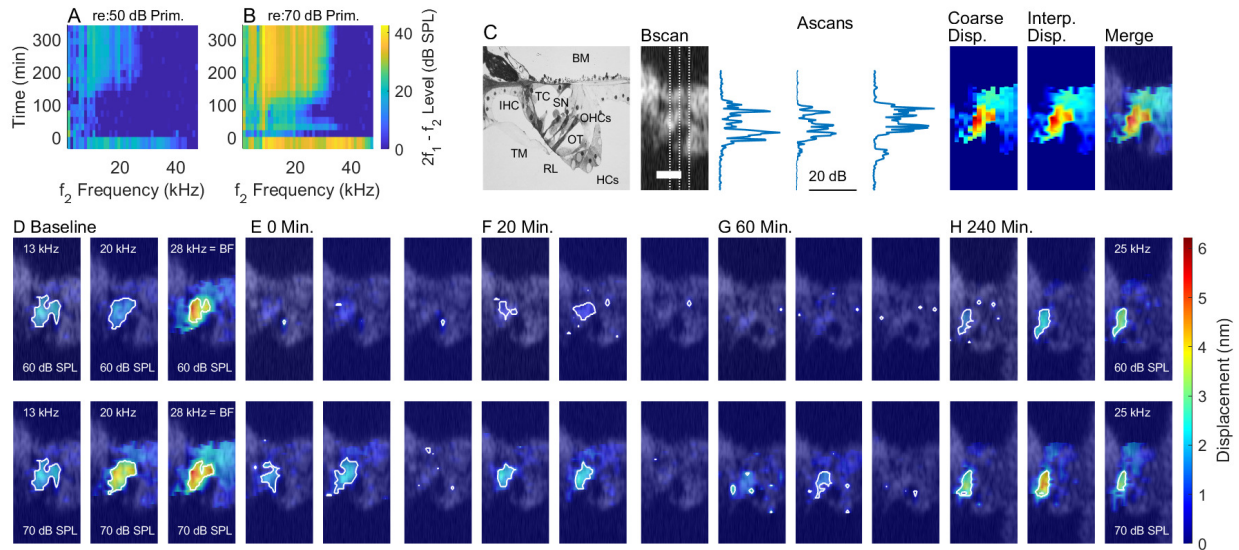


**FIGURE 1.** (A) and (B) show heat map plots of the DPOAE-grams measured in response to 50 and 70 dB SPL two tone stimuli before and after the administration of furosemide. In these plots the  $f_2$  frequency runs along the horizontal axis, time runs along the vertical axis, and the SPL of the  $2f_1 - f_2$  DPOAE level is indicated by the color bar at the right which applies to both panels. Prior the injection, this ear had robust DPOEAs which were abolished immediately after the injection (time  $t = 0$ ). The DPOAEs gradually recovered over the subsequent few hours, but the recovery was not monotonic at 70 dB. (C) Explanation of the method for obtaining the two-dimensional vibration maps. The left image is a micrograph of a guinea pig OCC with selected structures labeled: BM = basilar membrane, TM = tectorial membrane, OHCs = outer hair cells, IHC = inner hair cell, TC = tunnel of Corti, OT = outer tunnel, SN = space of Nuel, RL = reticular lamina, OT = outer tunnel, HCs = Hensen's cells. The image to the right is a Bscan centered around the OHC-region. The OHCs, tunnel of Corti, and outer tunnel are visible in this scan. Scale bar =  $50 \mu\text{m}$ . Time locked Ascans or Mscans were taken across the field of view in  $10 \mu\text{m}$  steps and the vibration amplitudes were determined at selected maxima in the Ascans. Three representative Ascans are shown to the right and were taken along the dashed lines in the Bscan. The vibration amplitudes as a function of position give the coarse displacement map at the right. Linear interpolation was then applied to this to give a heat map of the vibration amplitude with the same resolution, or number of pixels, as the imaging Bscan. Finally the heat maps are overlaid onto the Bscans to match the vibration amplitudes with structures in the OCC. (D–H) show vibration maps at three frequencies and two levels before (D) and at selected times after (E–H) IV furosemide and the loss of the EP. The amplitudes are indicated by the colorbar at the far right which applies to all displacement maps. At each time, pixels with the largest vibrations, within 2 standard deviations of the maximum, are outlined in white. Experiment #925, 10/13/2021.

## RESULTS

Fig. 1 shows loss and recovery of the DPOAEs and vibration responses following IV furosemide injection. The DPOAE-grams are shown as heat maps and the two-dimensional vibration maps show the amplitude of the axial vibrations across an approximately radial field of view at selected times before and after treatment. Following the injection and loss of EP, the DPOAEs evoked by the 50 dB primaries were abolished and those evoked by the 70 dB primaries were greatly reduced in amplitude. At 70 dB the DPOAEs showed a nonmonotonic recovery with a second stage of recovery beginning at about 120 minutes and recovery largely complete by 240 minutes.

Baseline vibrations showed a stereotyped pattern with the highest amplitudes focused in a narrow region, or “hot spot” using the terminology of Cooper *et al.* [8], extending through the bodies of the OHCs, from the base of the OHCs/Deiters' cell junctions to the RL. In the heat maps, pixels with the largest amplitudes, within two standard deviations of the maximum, are outlined in white to highlight the shape of the vibration patterns. At higher SPLs and at frequencies closer to the BF, the vibration patterns were more diffuse, showing substantial BM motion at points lateral to the intersection of the acute and pectinate zones (Fig. 1 D). Following the furosemide injection and subsequent loss of the EP, vibration amplitudes fell uniformly at all positions. In spite of the decreased amplitude, the vibrations remained strongest in the OHC region, as shown in Fig. 1 E taken right after the injection. Over the subsequent four hours, this cochlea showed unsteady recovery, with initial recovery at 20 minutes followed by a reduction at 60 minutes. Nonmonotonic recovery was also observed in the DPOAE as noted above, and in our previous furosemide studies, where nonmonotonicity was linked to shifts in MET operating point [1, 2]. At the 240

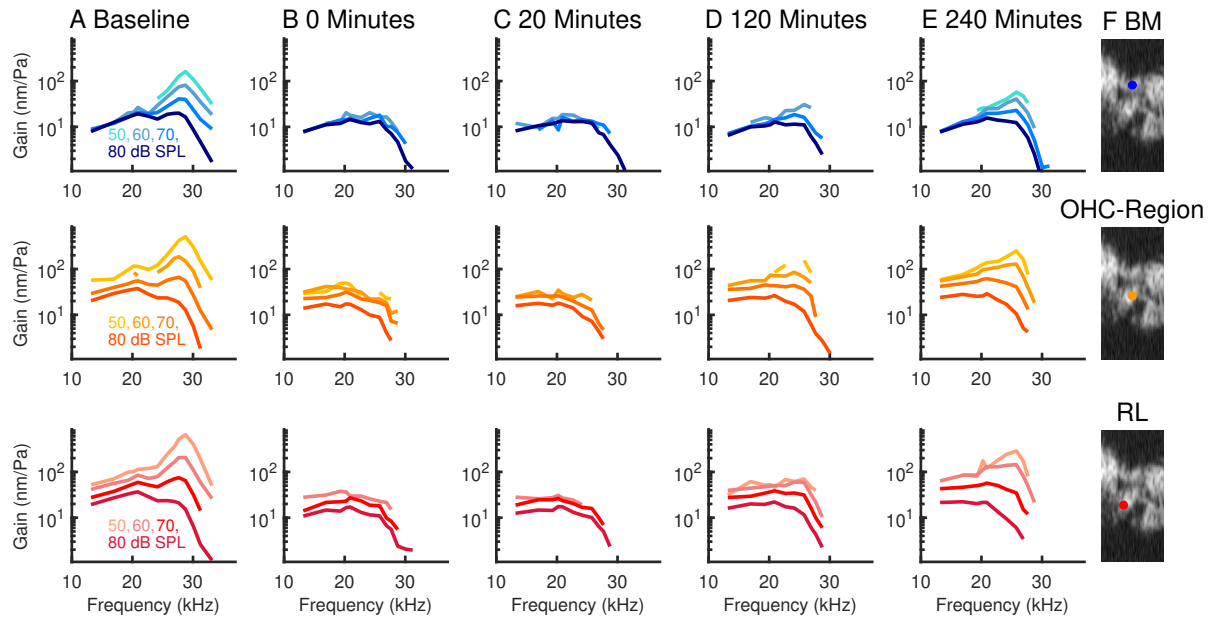


**FIGURE 2.** (A) – (F) Conventional tuning curves measured at the BM (top row, shades of blue), OHC-region (middle row, shades of orange), and RL, close to the apical surface of the OHCs, (bottom row, shades of red) before (A) and at selected times (B – E) after furosemide. Darker shades indicate higher SPLs and the times at the top of each column are the minutes that elapsed post treatment. Time  $t = 0$  in column (B) corresponds to recordings taken immediately after the injection. (F) The Bscans at the far right indicate the points on the OCC where the measurements were taken. Data are from the same experiment as Fig. 1.

minute mark, the vibration patterns had largely recovered to the baseline conditions, with the OHC-region having pre-treatment amplitudes. This preparation showed a somewhat delayed recovery relative to other individual experiments and a slightly reduced BF following recovery.

Fig. 2 shows tuning curves from the same experiment for three locations: the BM, the OHC-region, and the RL measured 20  $\mu\text{m}$  medial to the BM and OHC-region and close to the apical surface of the OHCs (see Bscans at right). The baseline vibrations were consistent with a healthy cochlea: the OHC-region and RL vibrations displayed higher amplitudes than the BM and a broad-band nonlinearity extending across all frequencies tested. Following the loss of the EP, the vibration amplitudes fell at all locations and the BM vibrations resembled those of a passive cochlea while the OHC-region and RL vibrations retained their broad-band nonlinearity. At around the 120 minute mark, the BF peak began to re-emerge and by 4 hours the vibrations appeared close to baseline levels.

The effects of salicylate on the areal vibration patterns were recently reported by our group [9] and are included to compare with the furosemide results that are newly reported here. Blocking somatic electromotility with extracellular salicylate likewise led to a reduction in the amplitudes at all points and a loss of the BF peak. Similar to the furosemide results, the BM responses appeared passive post-salicylate while the OHC-region and RL showed compressive growth for frequencies below BF. (See [9] for individual tuning curves.) In contrast to the treatment with furosemide, however, salicylate led to more qualitative changes in the vibration patterns. Post treatment, the vibrations were more diffuse and frequently showed large vibrations that were present in the lateral compartment of the OC, close to the Hensen's cells, as shown in Fig. 3 C and D. These vibrations appeared around 30 to 40 minutes after the salicylate was introduced into the perilymphatic space; could be greater in amplitude than the BM and OHC-region vibrations at the same time points (while having smaller amplitudes than the baseline vibrations); and were about as well tuned as the BM and OHC-vibrations at these times. As healthy responses recovered, these lateral vibrations faded and at the 200 minute time point, the strong OHC-region to BM axis of motion was again prominent.

Switching gears to the histological study of cochleae from furosemide-treated preparations, Fig. 4 shows scanning electron microscopy (SEM) images of OHC stereocilia bundles from the basal and middle turns. Control SEM images (Fig. 4 A–D) were taken from experiments without furosemide injection. Panels E–F depict the OHC bundles from the cochleae fixed between 20 – 40 minutes post furosemide. To date, results from the SEM images of the OHC

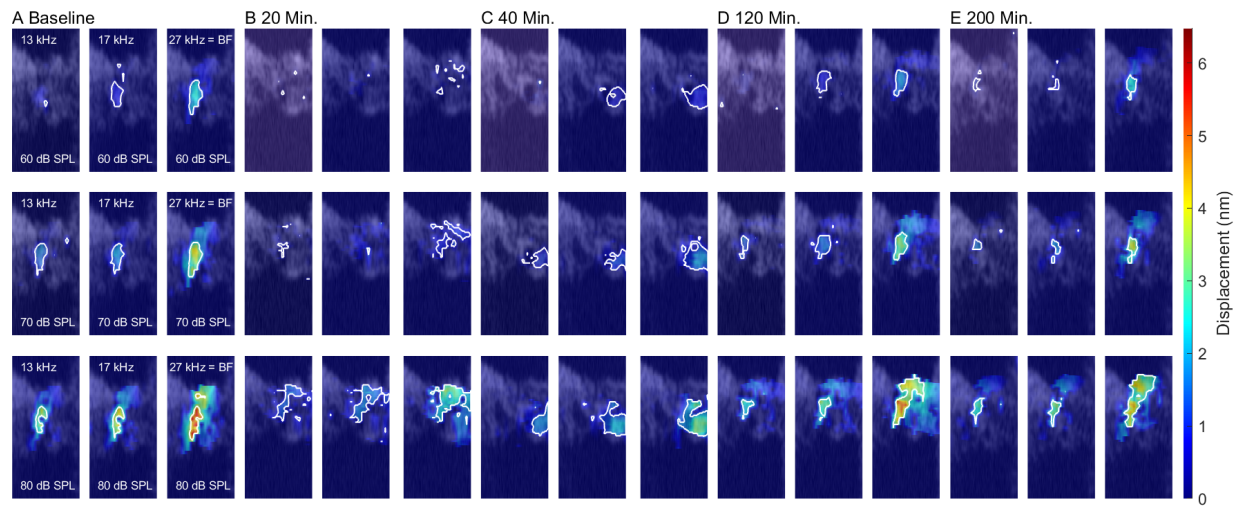


**FIGURE 3.** Effects of extracellular salicylate on two-dimensional vibration patterns. (A–E) Show vibrations shown at three frequencies and three levels before (A) and at selected times after (B – E) salicylate was introduced into scala tympani via diffusion across the round window membrane. Pixels with the largest vibrations, within 2 standard deviations of the maximum, are outlined in white. Similar to the loss of the EP due to furosemide, the vibrations show a loss of tuning and amplitude, but transiently show large vibrations in the lateral region, around the Hensen’s cells. These are particularly clear at the highest SPL (bottom row) in panels (B) and (C). These vibrations were present ~ 20 – 40 minutes post treatment and were not apparent at later times. Experiment #855, 12/15/2020. For more details see [9].

bundles after furosemide showed no consistent significant change in the morphology of the OHC stereocilia. In one case, we observed shortening at the first (shortest) row of the OHC stereocilia in the base (Fig. 4 F compared to Fig. 4 B). However, that result was not repeated in additional experiments.

## DISCUSSION

Changes in BM vibrations following intravenous furosemide [10] and perilymphatic perfusion of salicylates [11, 12] have been known since the 1990s but the effects on other structures within the OCC were unexplored until the advent of OCT and other depth-resolved interferometric techniques [13]. In the furosemide experiments, the complex loss and recovery of the active process following the drop and recovery of the EP suggest changes in the operating point of the hair cell mechano-electrical transduction (MET) complex, but the mechanism remains elusive [1, 2]. Using temporal bone explants, Jacob *et al.* showed that restoring EP led to micromechanical rearrangements in the OC and an increased gain relative to the passive, EP ~ 0 mV, system [14]. Changes in the resting position of the OHCs would alter the open probability of the MET channels and could explain these operating point shifts. The conformational changes observed in [14] were less than a few hundred nanometers, too small to be observed with an OCT in imaging mode where the resolution is on the order of a few microns. SEM imaging could theoretically observe at the 100-nanometer level, but in practice, processing-induced distortion would mask these conformational changes.

Using OCC explants, Vélez-Ortega *et al.* found that blocking normal transduction currents led to abnormal stereocilia lengths in the shorter two, or MET carrying, rows of OHC-bundles [4]. Eliminating the EP with furosemide will reduce the driving force for cation entry into the hair bundles and could lead to similar changes in the bundle morphology *in vivo*. Such changes would, in turn, alter the resting open probability of the MET channels at rest and could provide an explanation for the operating point shift we observed [1, 2]. Because bundle repair is a slow process, this could explain the slow and multiple time scales of the recovery we see post furosemide. However, the SEM studies did not uncover changes in stereocilia morphology following furosemide. Nevertheless, the SEM studies are just a single "snapshot", and it is possible that changes occurred or would have occurred before or after this snapshot (as was hinted in Fig. 4 F). While the findings here do not support the hypothesis that the stereocilia are involved in recovery following furosemide, they also do not disprove it. Continuous *in-vivo* imaging of stereocilia following furosemide would be useful to probe this hypothesis.

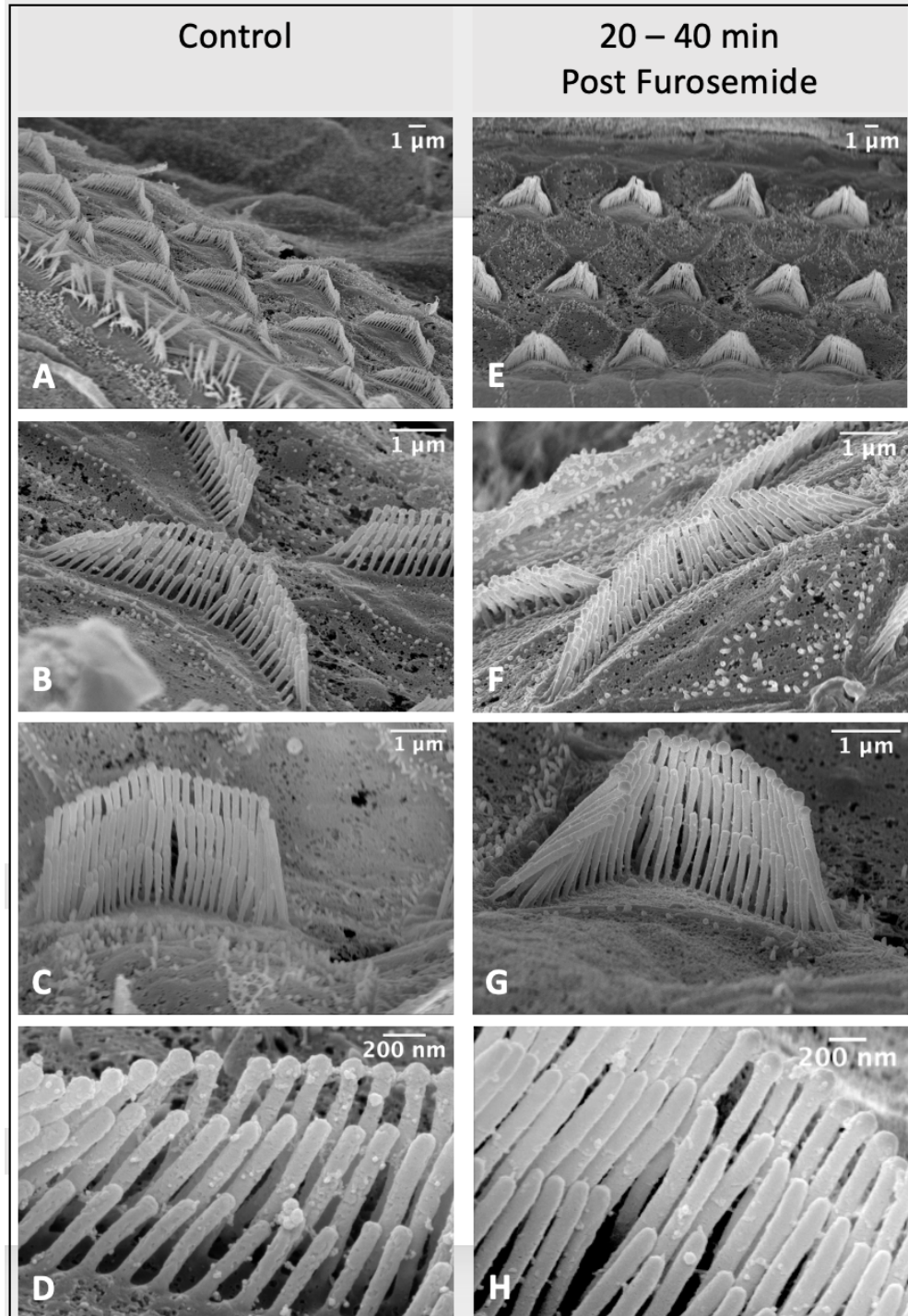


**FIGURE 4.** Scanning electron microscopy (SEM) images of OHC stereocilia bundles in gerbil. (A – D) from healthy cochlea (g919-LE). (A & B) Basal turn (C) Middle turn (D) Basal turn (apical end). (E – H) SEM images 20 – 40 minutes after IV injection of furosemide (g916-LE, g923-LE). (E & F) Basal turn. (G & H) Middle turn.

Perfusing salicylate into the perilymphatic space led to reduced amplitudes and a loss of the BF peak, similar to the effects with IV furosemide. Beyond that, salicylate changed the qualitative nature of the areal vibration patterns with the lateral compartment of the OC transiently exhibiting larger vibrations some 20 – 40 minutes post treatment but not at later times. These qualitative changes in the motion patterns would not be captured by single-location uniaxial measurements.

## CONCLUSIONS

The vibrations of the OCC are complicated, ultimately leading to the radial shearing motion between the reticular lamina and tectorial membrane that provides the mechanical input to the inner hair bundles' MET machinery, and hearing. Precisely how this shearing motion is generated, and how the active process or cochlear amplifier contributes to it is presently not well understood. The cochlea operates under feedback and determining the contributions of each component of the active process is challenging. Selective pharmacological blocking of individual elements of the cochlear amplifier *in vivo* sheds insight into how the elements of cochlear activity work in synchrony.

## ACKNOWLEDGMENTS

This work was supported by the NIDCD grant DC015362 and the Emil Capita Foundation.

## REFERENCES

1. Y. Wang, E. Fallah, and E. S. Olson, "Adaptation of cochlear amplification to low endocochlear potential," *Biophysical Journal*, Biophysical Journal **116**, 1769–1786 (2019).
2. C. E. Strimbu, Y. Wang, and E. S. Olson, "Manipulation of the endocochlear potential reveals two distinct types of cochlear nonlinearity," *Biophysical Journal*, Biophysical Journal **119**, 2087–2101 (2020).
3. B. L. Frost, C. E. Strimbu, and E. S. Olson, "Using volumetric optical coherence tomography to achieve spatially resolved organ of Corti vibration measurements," *J Acoust Soc Am* **151**, 1115 (2022).
4. A. C. Véllez-Ortega, M. J. Freeman, A. A. Indzhukulian, J. M. Grossheim, and G. I. Frolenkov, "Mechanotransduction current is essential for stability of the transducing stereocilia in mammalian auditory hair cells," *eLife* **6**, e24661 (2017).
5. N. C. Lin, C. E. Strimbu, C. P. Hendon, and E. S. Olson, "Adapting a commercial spectral domain optical coherence tomography system for time-locked displacement and physiological measurements," *AIP Conference Proceedings* **1965**, 080004 (2018), <https://aip.scitation.org/doi/pdf/10.1063/1.5038488>.
6. E. Fallah, C. E. Strimbu, and E. S. Olson, "Nonlinearity and amplification in cochlear responses to single and multi-tone stimuli," *Hearing Research* **377**, 271–281 (2019).
7. I. I. Sadreev, G. W. S. Burwood, S. M. Flaherty, J. Kim, I. J. Russell, T. I. Abdullin, and A. N. Lukashkin, "Drug Diffusion Along an Intact Mammalian Cochlea," *Front Cell Neurosci* **13**, 161 (2019).
8. N. P. Cooper, A. Vavakou, and M. van der Heijden, "Vibration hotspots reveal longitudinal funneling of sound-evoked motion in the mammalian cochlea," *Nat Commun* **9**, 3054 (2018).
9. C. E. Strimbu and E. S. Olson, "Salicylate-induced changes in organ of corti vibrations," *Hearing Research*, 108389 (2021).
10. M. A. Ruggero and N. C. Rich, "Furosemide alters organ of corti mechanics: evidence for feedback of outer hair cells upon the basilar membrane," *J Neurosci* **11**, 1057–1067 (1991).
11. E. Murugasu and I. J. Russell, "Salicylate ototoxicity: The effects on basilar membrane displacement, cochlear microphonics, and neural responses in the basal turn of the guinea pig cochlea," *Auditory Neuroscience* **1**, 139–150 (1995).
12. J. Santos-Sacchi, L. Song, J. Zheng, and A. L. Nuttall, "Control of mammalian cochlear amplification by chloride anions," *Journal of Neuroscience* **26**, 3992–3998 (2006).
13. T. Ren, W. He, and P. G. Barr-Gillespie, "Reverse transduction measured in the living cochlea by low-coherence heterodyne interferometry," *Nat Commun* **7**, 10282 (2016).
14. S. Jacob, M. Pienkowski, and A. Fridberger, "The endocochlear potential alters cochlear micromechanics," *Biophys J* **100**, 2586–2594 (2011).